infrastructures

MDPI

Article

Engineering Challenges for Safe and Sustainable Underground Occupation

Maria do Carmo Reis Cavalcanti [1,*], Wagner Nahas Ribeiro [1,*] and Marcelo Cabral dos Santos Junior [2]

[1] Escola Politécnica, Universidade Federal do Rio de Janeiro, Rio de Janeiro 21941-901, RJ, Brazil
[2] Coba, Rio de Janeiro 21941-901, RJ, Brazil
* Correspondence: carminhacavalcanti@poli.ufrj.br (M.d.C.R.C.); wagnernahas@poli.ufrj.br (W.N.R.)

Abstract: Shallow tunnels induce surface displacements which can cause damage to existing structures; an adequate evaluation of their settlement trough is of paramount importance. Nowadays, it becomes even more critical when dealing with an underground occupation where the green stress field has already been disturbed by previous excavations. Since the end of the last century, many researchers have explored the subject. Some empirical methodologies have been developed based on data from actual cases, sometimes associated with numerical analysis. The present work used plane strain numerical analysis of different geometric arrangements of side-by-side twin tunnels for different depths and distances between tunnel axes to evaluate its compatibility with some of the proposed methods to adjust the settlement profile of the second cavity. It was observed that the discussed methodologies have similar results for maximum settlement and its eccentricity. Nevertheless, the behavior of the trough width parameter from the semi-empirical methods has shown discrepancies.

Keywords: tunnels; side-by-side twin tunnels; settlement trough; numerical analysis; finite element method

Citation: Cavalcanti, M.d.C.R.; Nahas Ribeiro, W.; Cabral dos Santos Junior, M. Engineering Challenges for Safe and Sustainable Underground Occupation. *Infrastructures* **2023**, *8*, 42. https://doi.org/10.3390/infrastructures8030042

Academic Editor: Paolo Simonini

Received: 19 December 2022
Revised: 2 February 2023
Accepted: 10 February 2023
Published: 27 February 2023

1. Introduction

World population growth and socioeconomic development have generated an increasing demand for space for housing, socioeconomic activities, and the necessary infrastructure to support them. Surface space in metropolitan areas has invaluable importance but also does an optimized transport and public utility systems, which led to underground solutions such as subway tunnels and road passages as well as buried pipes for drainage, sewage, and cables in general, among other facilities.

Shallow underground excavations induce surface displacements in their vicinity, which can cause damage to buildings and other existing underground structures. Therefore, an adequate evaluation of the settlement trough above shallow tunnels is of great importance in the design of any subterranean project.

It becomes even more critical in a crowded underground space where the media stress field has already been disturbed by previous excavations, and additional cavities cause more significant displacements than the ones carried out in a green stress field.

Analysis of surface settlement due to tunneling is a complex phenomenon, and there are numerous research papers on ground settlement due to tunnel construction, including theoretical analysis methods, numerical simulations, field measurements, and other methods of analyzing the mechanism of ground deformation caused by the excavation process.

Peck [1] proposed a theoretical method, based on a statistical analysis of a large amount of monitoring data, for the ground settlement caused by a single tunnel, assuming that the volume of the settlement trough was equal to the volume loss of the excavated cross-section of the cavity and had a distribution analogous to a Gaussian curve as shown on Figure 1 and defined by Equation (1):

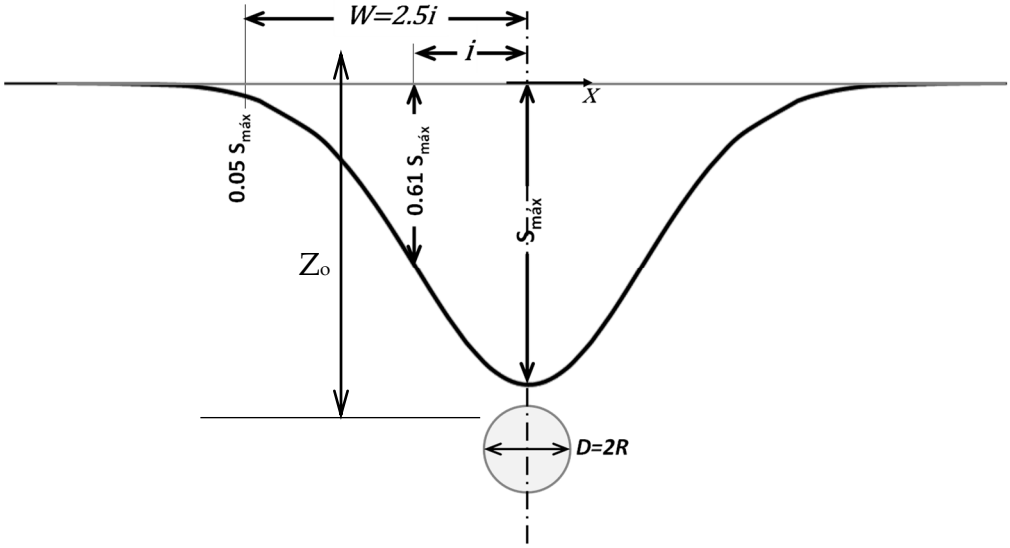

Figure 1. Settlement trough.

$$S(x) = S_{max}.e^{\left(\frac{-x^2}{2i^2}\right)} \quad (1)$$

where:

$S(x) \rightarrow$ settlement at a distance "x" from the tunnel centerline;

$S_{max} \rightarrow$ maximum settlement above the tunnel centerline;

$i \rightarrow$ Gaussian curve point of inflection (corresponding to the standard deviation of the Gaussian distribution curve), which depends on the ground conditions; and

$x \rightarrow$ distance from the tunnel center line.

Peck's formula has become a generally accepted model for estimating the settlement trough over a single tunnel; on the other hand, as presented in Table 1, the trough width "i" parameter has deserved much more attention (Attewell et al. [2], Atkinson and Potts [3], Clough and Schmidt [4], O'Reilly and New [5], Mair [6], Mair and Taylor [7]).

Table 1. Inflection dimension proposed by various researchers.

Author	*i* Value
Peck [1]	$\frac{i}{R} = \left(\frac{Z_o}{2R}\right)^n$ where n = 0.8 to 1.0
Attewell et al. [2]	$\frac{i}{R} = \propto \left(\frac{Z_o}{2R}\right)^n$ where α = 1 and n = 1.0
Atkinson and Potts [3]	$i = 0.25\ (Z_o + R)$ loose sand $i = 0.25\ (1.5Z_o + 0.5R)$ dense sand/over consolidated clay
Clough and Schmidt [4]	$\frac{i}{R} = \propto \left(\frac{Z_o}{2R}\right)^n$ where α = 1 and n = 0.8
O'Reilly and New [5]	$i = 0.43Z_o + 1.1$ cohesive soil $i = 0.28Z_o - 0.1$ granular soil
Mair [6]	$i = 0.5Z_o$
Mair and Taylor [7]	$i = KZ_o$ K_{clays} = 0.4 a 0.5 and K_{sand} = 0.25 a 0.45

Zo = depth of tunnel axis below ground surface. R = tunnel radius.

New and O'Reilly [8] complemented Peck's concept for two and multiple tunnels proposing that the final settlement profile can be obtained by adding the individual Gaussian curves of each cavity based on the assumption that the tunnels would behave as if the others did not exist, not accounting for the fact that usually excavations are not carried out simultaneously. Equation (2) represents the proposed methodology for twin tunnels

where the "x" coordinate refers to one of the tunnels, and "L" is the distance between the cavity's axes:

$$S(x) = S_{max} \cdot \left\{ e^{\left(-\frac{x^2}{2i^2}\right)} + e^{\left(-\frac{(x-L)^2}{2i^2}\right)} \right\} \quad (2)$$

where:

$x \rightarrow$ distance from the center line of one of the twin tunnels;

$L \rightarrow$ distance between the tunnels' axes.

Nevertheless, based on field data, many authors reported discrepancies in the settlement profile when the second tunnel excavation was carried out. Terzaghi [9] declared that ground movements caused by the second tunnel were more significant than those caused by the first. Moretto [10] also observed larger settlements for the second of twin tunnels constructed in dense silty sand, overlying firm clay. Cording and Hansmire [11] reported an increase in surface displacements above the 6 m diameter Washington subway second twin tunnels. Akins and Abramson [12] observed more significant volume loss for the second twin tunnels, 6.1 m in diameter and center-to-center spacing of 6 m, constructed at a depth of 15 m in residual soil.

Mair and Taylor [7] attributed the changes in settlement above the second tunnel to the fact "that the soil has been previously strained by tunnel one and bigger volume losses would be expected for tunnel 2". Chapman et al. [13] defined a deformation 'overlapping zone' that accounts for the observed behavior due to stress field disturbance from excavating the first tunnel.

Addenbrooke and Potts [14,15] carried out a series of plane strain finite element analyses, simulating twin tunnel behavior driven in stiff clay with high Ko, with nonlinear elastic perfectly plastic constitutive models and coupled consolidation, considering a typical London soil profile. Two geometries with parallel tunnels were studied, one with both tunnels at the same depth and another where both had the same vertical axis; different spacings between the cavities were evaluated, as well as the period between the excavations.

Addenbrooke and Potts [14,15] concluded that the spacing of the two tunnels affects the ground surface, whether the tunnels are side-by-side or one above the other, tending to it as the distance between the tunnels increase. For the side-by-side configuration, the shape of the settlement troughs above each of the second tunnels is very similar to the greenfield profile, but the lateral position of the maximum settlement moves from its center line toward the existing tunnel. As for the piggyback configuration, the shape of the settlement troughs of the second tunnel is flatter and broader than the greenfield profile.

In agreement with Addenbrooke and Potts [14,15] conclusions, Cooper et al. [16] and Chapman et al. [13] reported that field data, as well as numerical modeling, have shown, for side-by-side twin tunnels, an asymmetry in the second tunnel settlement profile, with more significant values occurring on the side closer to the first cavity.

To account for such asymmetry and values of the second tunnel settlement trough, Chapman et al. [13] proposed a correction factor *F(x)*, defined by Equation (3), to be applied to the overlapping zone settlement profile of the second tunnel according to Equations (4) and (5), Figure 2 shows twin tunnels settlement trough for the proposed methodology along with the one from O'Reilly and New [8].

$$F(x) = \left\{ 1 + \left[M \left(1 - \frac{|L + x|}{A.i} \right) \right] \right\} \quad (3)$$

$$\text{Overlapping zone}: \; S_2(x) = F(x).S_1^{max}.e^{\frac{-x^2}{2i_1^2}} \quad (4)$$

$$\text{Outside overlapping zone}: \; S_2(x) = S_1^{max}.e^{\frac{-x^2}{2i_1^2}} \quad (5)$$

where:

$F(x)$ = correction factor;
M = Maximum modification (e.g., 60% = 0.6);
x = distance to the axis of the first tunnel;
L = distance between tunnel axes;
i = trough width parameter of the first tunnel (m);
A = Multiple of (i) for half trough width (typically 2.5 or 3.0);
S_1^{max} = maximum settlement of the first tunnel excavated;
$S_2(x)$ = settlement trough of the second tunnel excavated.

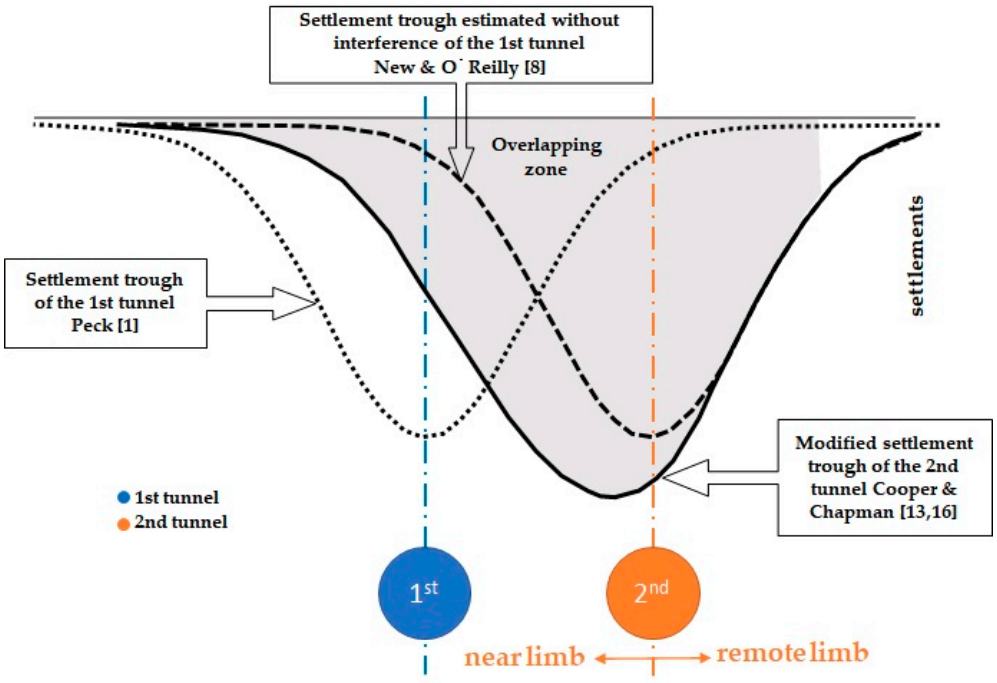

Figure 2. Twin tunnels settlement trough.

Cording and Hansmire [11] have suggested that the trough width of side-by-side twin tunnels could increase for the second tunnel on the side near the first tunnel driven. Cooper and Chapman [16] provided a way for estimating the relative increases in the settlement trough width based on an increase in the volume of the near limb, V_{2n}, relative to the remote limb, V_{2r}. The volume and hence the half trough width of the near limb were assumed to be greater than that of the remote limb, considering different values of i in the correction factor for each limb of the second tunnel profile, i_n (near limb) > i_r (remote limb). Incorporating the methodology proposed by Chapman et al. [13], Equations (4) and (5) could be written as Equations (6)–(9).

Overlapping zone: $L\text{-}A.i_2 < x < Ai_1$

$$\text{near limb}: \; S_{2_n}(x) = F(x).S_1^{max}.e^{\frac{-x^2}{2i_n^2}} \tag{6}$$

$$\text{remote limb}: \; S_{2_r}(x) = F(x).S_1^{max}.e^{\frac{-x^2}{2i_r^2}} \tag{7}$$

Outside overlapping zone: $L\text{-}A.i_2 > x > Ai_1$

$$\text{near limb}: \; S_{2_n}(x) = S_1^{max}.e^{\frac{-x^2}{2i_n^2}} \tag{8}$$

$$\text{remote limb}: \; S_{2_r}(x) = S_1^{max}.e^{\frac{-x^2}{2i_r^2}} \tag{9}$$

where:

x = distance to the axis of the first tunnel;

$S_{2n}(x)$ = second tunnel settlement in the near limb region, between tunnel axes and beyond;

$S_{2r}(x)$ = second tunnel settlement in the remote limb region, from the second tunnel axes in the opposite direction;

i_n = trough width parameter for the near limb settlement curve;

i_r = trough width parameter for the remote limb settlement curve.

Ocak [17], based on surface settlement monitoring data from the 6.5 m diameter twin tunnels of the Otogar-Kirazlı metro, driven by EPBM, proposed a second tunnel settlement trough adjustment based on the distance between the cavities' axes. The methodology accounts for the increase in volume and width of the second tunnel profile; nevertheless, it does not contemplate the near limb/remote limb asymmetry.

This procedure makes use of a factor to increase the maximum settlement as well as the trough width parameter "i", as described by Equations (10)–(12):

$$i_2 = k.i_1 \tag{10}$$

$$S_2^{max} = k.S_1^{max} \tag{11}$$

$$k = 1 + {}^{D}/_{L} \tag{12}$$

where:

k = adjusting factor;

D = tunnel diameter;

L = distance between tunnel axes;

i_1 = settlement trough width parameter for the first tunnel excavated;

i_2 = settlement trough width parameter for the second tunnel;

S_1^{max} = maximum settlement of the first tunnel excavated;

S_2^{max} = maximum settlement of the second tunnel.

Recently, probabilistic (Qi and Zhou [18] and Zhou et al. [19]) and machine learning (Suwansawat and Einstein [20], Chen et al. [21], Cheng et al. [22,23]) methods have also emerged as an efficient way to tackle complex geotechnical problems including tunneling-induced settlements.

After this paper had been written, Gao et al. [24] published a settlement trough alternative formulation for sands and gravel based on 138 groups of measured data of land subsidence between Mudan Dadao station and Longmen Dadao station of Metro Line 2.

2. Materials and Methods

The present work intended to validate the applicability and limitations of a FEM analysis of shallow excavations that does not demand support and without the presence of water, comparing its results, for multiple depths and distances between twin tunnels, with the ones from the methodologies proposed by Cooper and Chapman and Ocak detailed previously.

Both semi-empirical formulations were based on and validated by field data from TBM excavations, which would mainly influence the volume lost value. Furthermore, the type of material would affect the trough width parameter "i". Once the present evaluation focused on the behavior of the second tunnel settlement profile, the influence of such empirical parameters was avoided by means of considering, in the semi-empirical formulations, the maximum settlement and trough width parameter obtained from the first tunnel numerical analysis profile.

This work's numerical analyses were developed using the finite element 2D stress–strain module SIGMA/W of GEOSLOPE International Ltd. (Calgary, AB, Canada) GeoStudio 2021.3 package.

2.1. Geometry and Soil Parameters

The studied geometry consists of side-by-side circular twin tunnels 5 m in diameter excavated in clay soil with no water presence.

The study contemplated four depths (12.5 m, 17.5 m, 22.5 m, 27.5 m) and four distances between axes (10 m, 15 m, 20 m, and 25 m), totaling 16 analyses.

The soil parameters are those from one of the clay layers present in the Istanbul stations area, as described by Ocak [17], and are presented in Table 2.

It was assumed, for all purposes, that the soil had enough strength to be self-supporting, and no support was considered in the analyses.

Table 2. Soil properties.

Soil Type	**Clay**
Constitutive model	Isotropic linear elastic
Young's module	20 MPa (constant)
Poisson	0.35
Specific weight	16.5 kN/m^3

2.2. Finite Element Model and Analyses

The finite element mesh for all studied geometries is 120 m wide and 60 m deep, ensuring a distance between the tunnel's contour and model limits of at least six times the tunnel diameter to minimize border effects.

The vertical borders of the model had the horizontal displacements restricted, the inferior border had the vertical displacements restrained, and the superior edge had no restriction.

The mesh was divided into six regions for adequate refinement in the region of interest, and with the following characteristics:

- Three- and four-node elements;
- Refined region around cavities, 24 nodes in each tunnel (regions 2 and 3);
- One meter elements on the surface (region 1);
- Lateral regions (4 and 5) 2 m elements on the surface;
- Bottom region (6) 2.5 m elements.

The analysis of each geometric configuration has been carried out as follows:

1. No excavation and gravitational load to establish the greenfield stresses;
2. Excavation of the first tunnel;
3. Excavation of the second tunnel.

2.3. Methodology

The flowchart presented in Figure 3 resumes the methodology followed in the present study, where each geometry, characterized by 16 combinations of depth and distance between the side-by-side twin tunnels, is compared to the methods proposed by Cooper and Chapman [16] and Ocak [17].

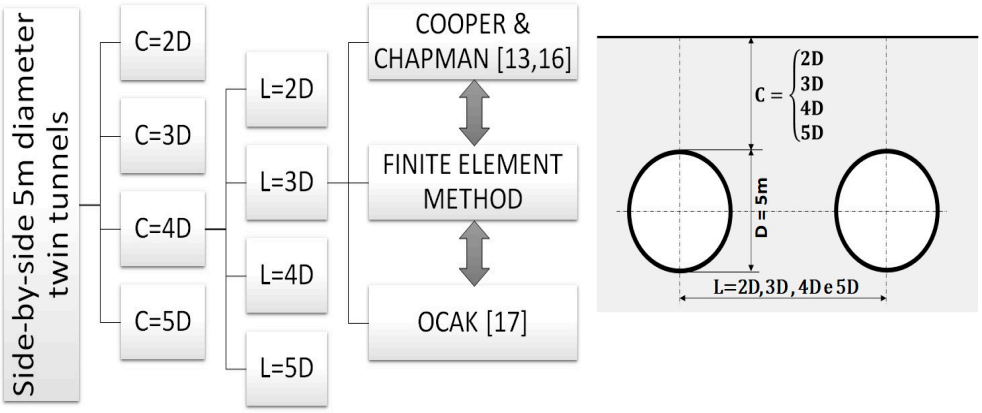

Figure 3. Comparison methodology.

Figure 4 summarizes the procedure adopted for each geometry to calculate the second tunnel empirical settlement trough.

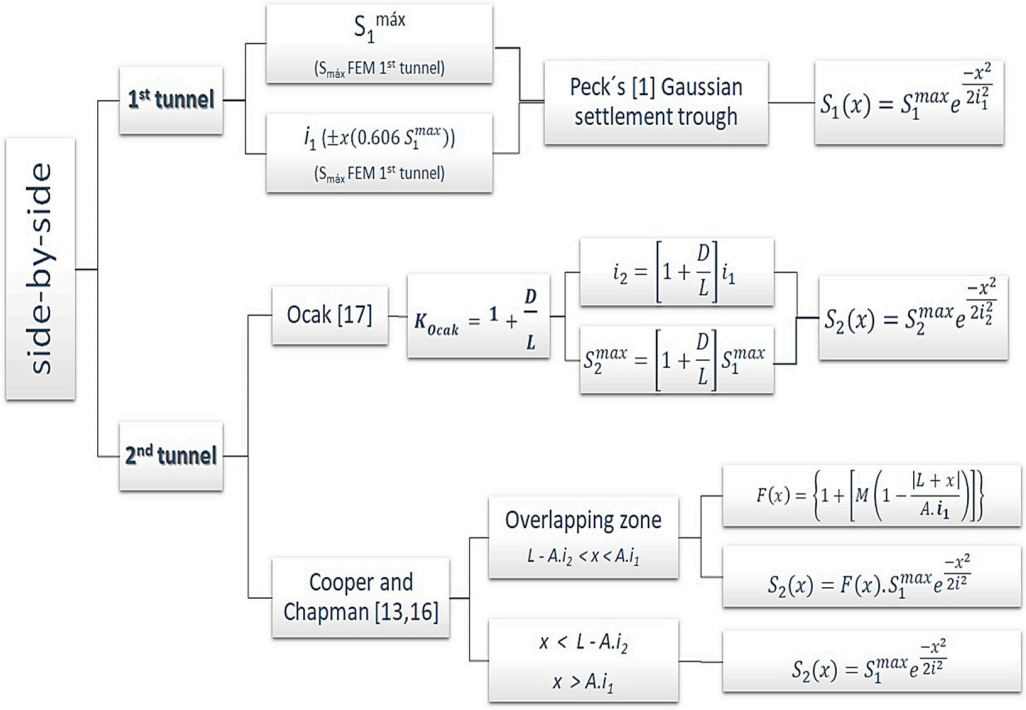

Figure 4. Semi-empirical settlement trough calculation procedure.

3. Results

The settlement troughs from the numerical analyses are presented in Figure 5, where besides the influence of the distance between the cavities on the increase in the maximum settlement of the second tunnel as well as its movement from the second tunnel axis towards the first tunnel as established in the literature on the subject can be observed.

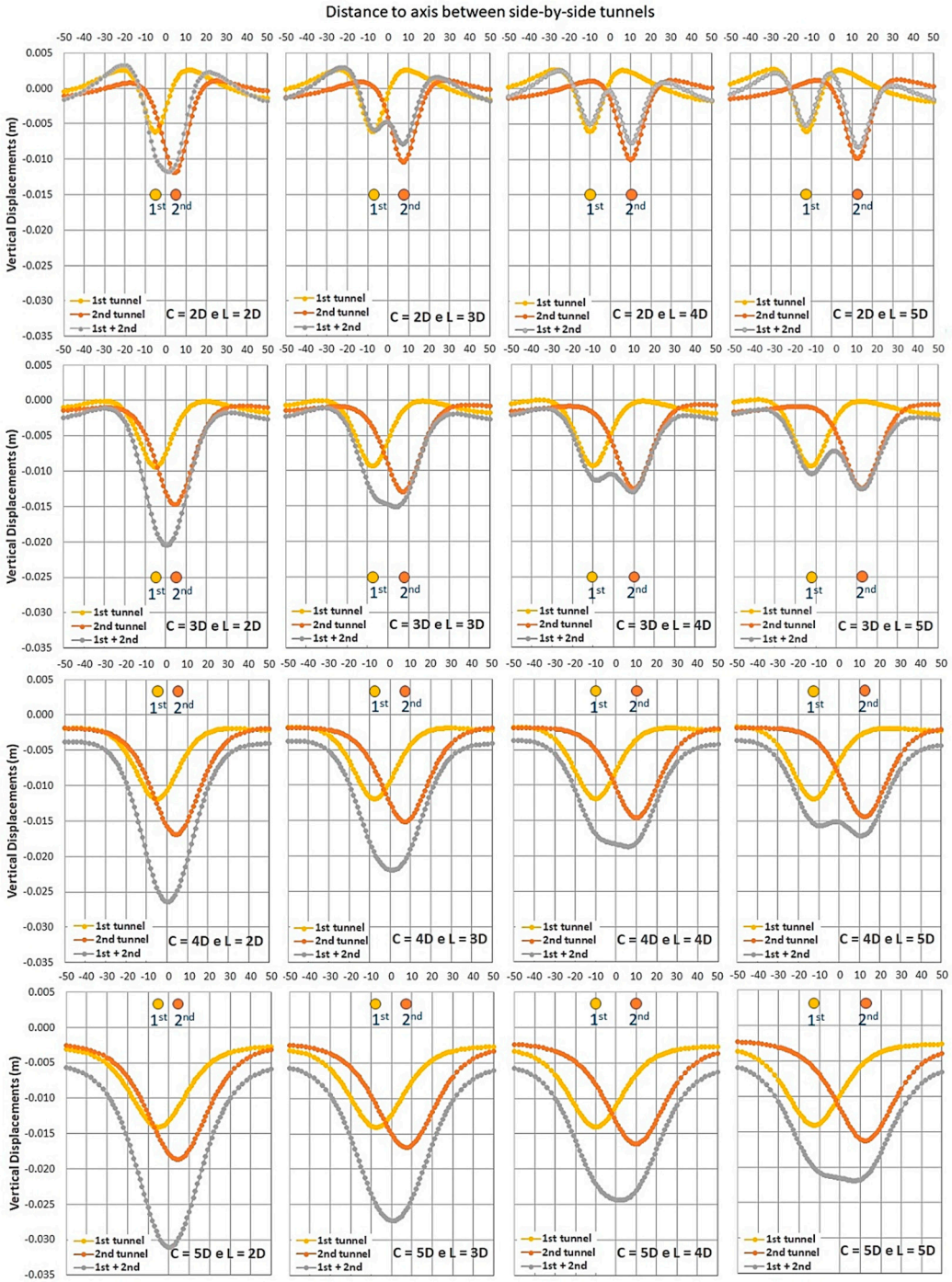

Figure 5. Numerical analysis settlement troughs.

It can also be seen in Figure 5 that, for the shallower tunnels (C = 2D) geometries, the first cavity settlement profile shows upward movements on the surface, which was also observed in the analyses and field measurements presented by Zhao et al. [25].

The maximum settlements and their normalized values with the soil coverage (C) are presented in Table 3 for both tunnels and all 16 configurations.

Table 3. Numerical analyses of maximum settlement.

Geometric Configuration		1st Tunnel Trough		2nd Tunnel Trough	
L [(1)]/D	C [(2)]/D	S_1^{max} (m)	S_1^{max}/C	S_2^{max} (m)	S_2^{max}/C
2	2	−0.00618	−0.0006	−0.01190	−0.0012
2	3	−0.00610	−0.0006	−0.01038	−0.0010
2	4	−0.00611	−0.0006	−0.00999	−0.0008
2	5	−0.00607	−0.0006	−0.00990	−0.0007
3	2	−0.00942	−0.0006	−0.01474	−0.0010
3	3	−0.00936	−0.0006	−0.01296	−0.0009
3	4	−0.00935	−0.0006	−0.01256	−0.0008
3	5	−0.00932	−0.0006	−0.01241	−0.0007
4	2	−0.01192	−0.0006	−0.01688	−0.0010
4	3	−0.01193	−0.0006	−0.01519	−0.0008
4	4	−0.01190	−0.0006	−0.01462	−0.0007
4	5	−0.01190	−0.0006	−0.01448	−0.0007
5	2	−0.01412	−0.0006	−0.01865	−0.0010
5	3	−0.01408	−0.0006	−0.01691	−0.0008
5	4	−0.01403	−0.0006	−0.01645	−0.0007
5	5	−0.01408	−0.0006	−0.01624	−0.0006

[(1)] distance between tunnel axes. [(2)] soil coverage.

An aspect not discussed in previous works is the tunnel depth influence in the second excavation settlement profile; Figure 6 shows that such effect decreases with the cavities' depth and has little impact on the first tunnel maximum settlement ratio (S_{max}/C).

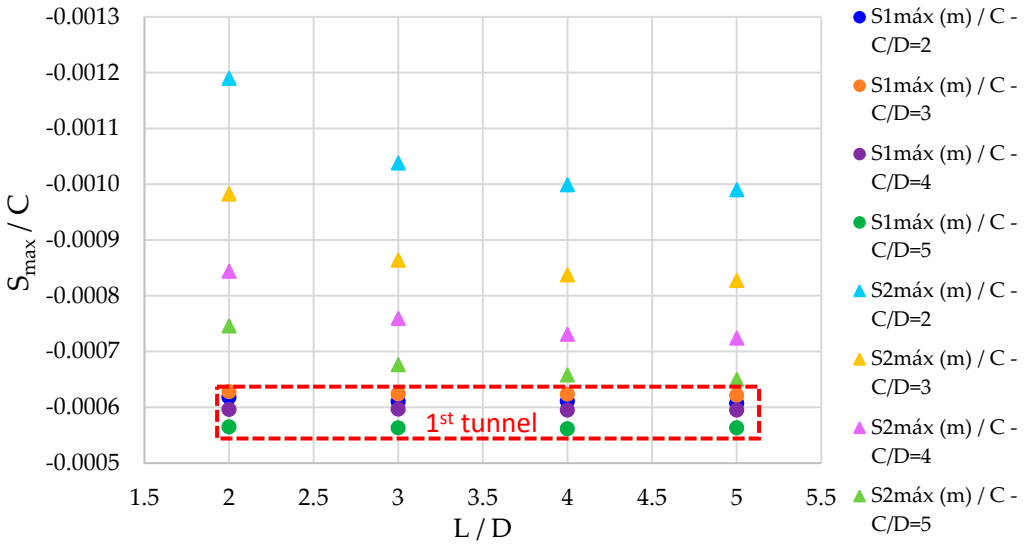

Figure 6. Geometry influence on the maximum settlement.

Cooper and Chapman [16], as well as Ocak [17], report differences in the width of the settlement trough for the second tunnel; therefore, it was carried out an evaluation of the finite element vertical displacement curves in what concerns such aspect.

The trough width is defined by the parameter "*i*", which represents the inflection point of the Gaussian curve corresponding to a percentage of 60.6% of the maximum settlement. Nevertheless, the numerical curve inflection points, where the second derivatives of S(x)

are zero, do not correspond to 60.6% of the maximum settlement. Therefore, the ratio "i_2/i_1" was evaluated independently for each hypothesis, as presented in Table 4 and Figure 7.

Table 4. Numerical analyses settlement trough.

Geometric Configuration		FEM $i = x\ (d^2S/dx^2 = 0)$ [3]			FEM $i = x\ (S = 0.606S_{max})$		
C [2]/D	L [1]/D	i_1 (m)	i_2/i_1	i_2 (m)	i_1 (m)	i_2/i_1	i_2 (m)
2	2	5.26	1.06	5.55	4.26	1.35	5.74
2	3	5.24	1.04	5.43	4.26	1.28	5.44
2	4	5.25	1.04	5.47	4.24	1.26	5.35
2	5	5.25	1.04	5.44	4.25	1.26	5.35
3	2	7.32	1.08	7.89	7.62	1.18	8.97
3	3	7.31	1.04	7.59	7.63	1.14	8.68
3	4	7.31	1.03	7.56	7.60	1.13	8.55
3	5	7.29	1.03	7.51	7.60	1.12	8.52
4	2	9.45	1.07	10.15	11.37	1.08	12.31
4	3	9.44	1.04	9.85	11.37	1.07	12.20
4	4	9.45	1.04	9.80	11.38	1.06	12.09
4	5	9.32	1.08	10.06	11.38	1.06	12.06
5	2	11.72	1.06	12.43	15.39	1.02	15.75
5	3	11.80	1.04	12.25	15.41	1.03	15.84
5	4	11.75	1.05	12.38	15.44	1.03	15.84
5	5	11.11	1.05	11.66	15.45	1.02	15.81

[1] distance between tunnel axes. [2] soil coverage. [3] second derivatives from first-order finite difference.

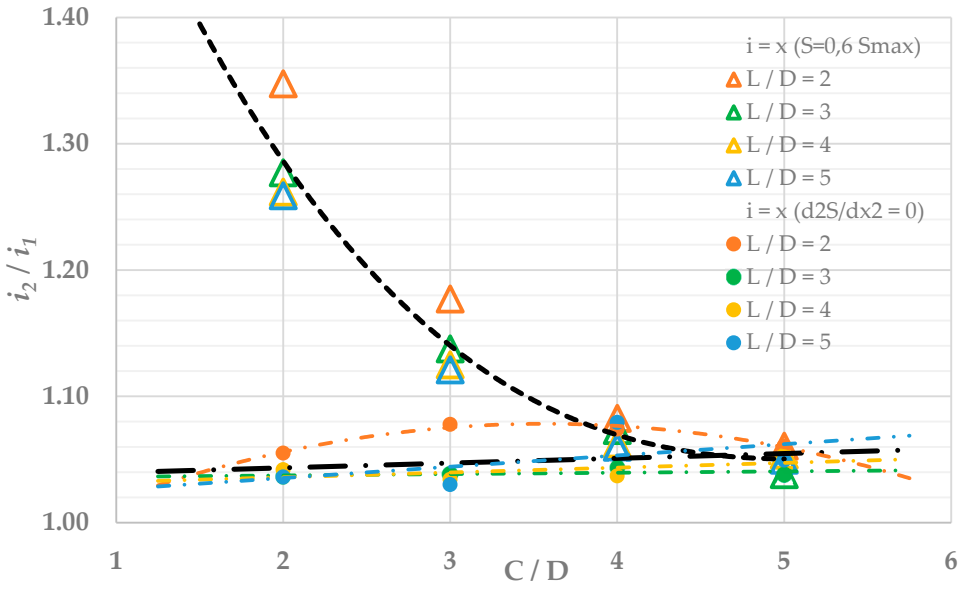

Figure 7. Geometry influence on the settlement trough the width.

The ratio i_2/i_1 considering 60% of the maximum settlement, shows much bigger values and decreases drastically as depth increases, while the second derivative values vary from 1.03 to 1.08; both seem to converge to a constant value around 1.05 for C/D > 5.

4. Discussion

To compare the results from the numerical analysis with the methodologies proposed by New and O'Reilly [8], Cooper and Chapman [16], and Ocak [17]; the settlement troughs of each procedure are presented in Figure 8.

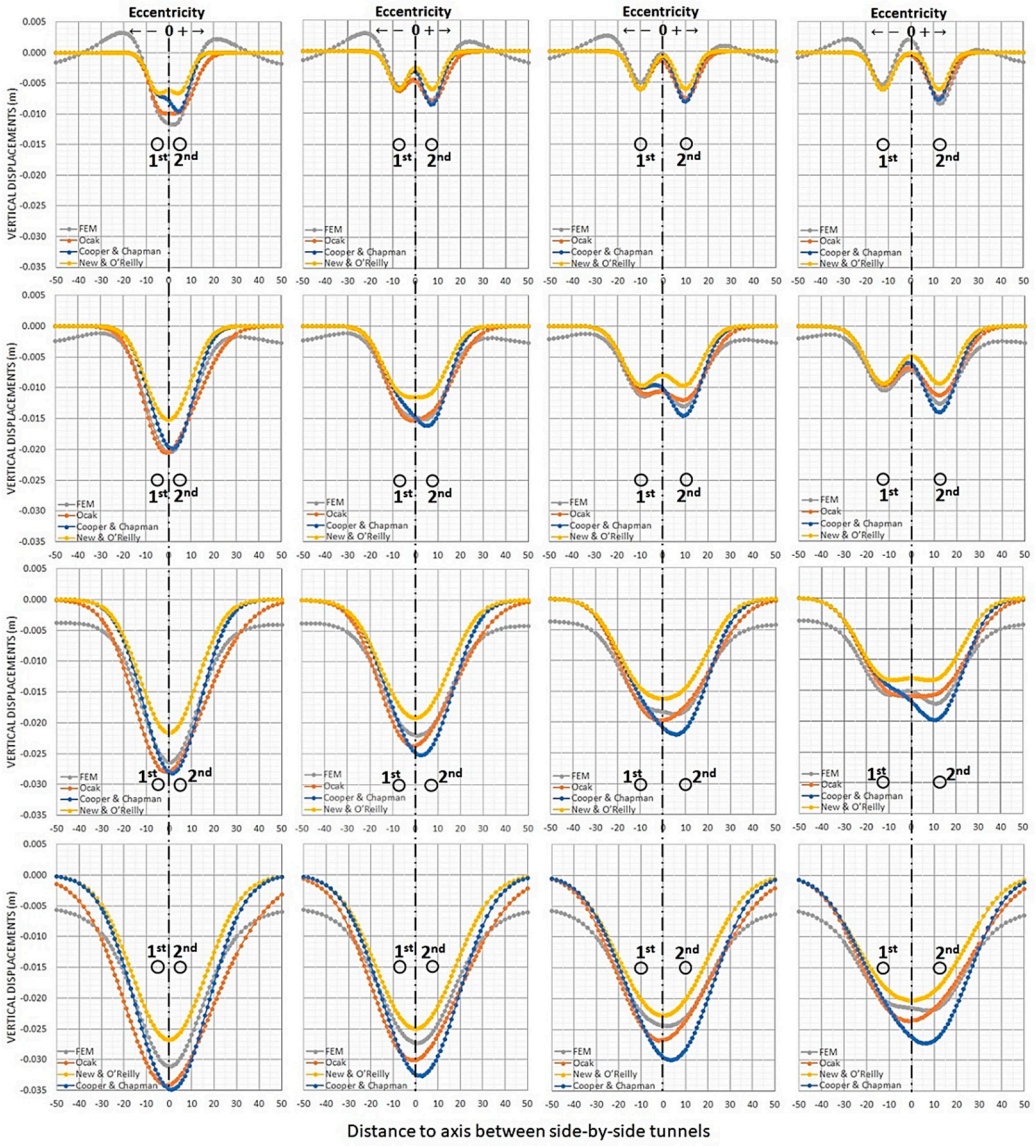

Figure 8. Settlement troughs for the different methodologies.

The settlement troughs from New and O'Reilly [8] are symmetrical to the axis between tunnels and present the smaller values of the maximum settlement; all other methodologies show eccentricity of the maximum settlement with more significant maximum values.

The effect of geometry (depth and distance between tunnels) on maximum settlement, eccentricity, and trough width (i) was evaluated for the methodologies that return asymmetrical settlement troughs.

Table 5 presents the maximum settlement and eccentricities for such methodologies, along with the values from FEM analysis, where are considered positives the eccentricities towards the second cavity and negative in the opposite direction in relation to the axis at mid-distance from the tunnels.

$$eccentricity \rightarrow \begin{cases} (+) \rightarrow towards\ the\ 2^{nd}\ tunnel \\ (-) \rightarrow towards\ the\ 1^{st}\ tunnel \end{cases}$$

Table 5. The eccentricity of the maximum settlement.

Geometric Configuration		$S_{máx}$ (m)			Eccentricity [3] (m)		
C [2]/D	L [1]/D	Cooper and Chapman	Ocak	FEM	Cooper and Chapman	Ocak	FEM
2	2	−0.0096	−0.0099	−0.0117	4.0	2.0	2.0
2	3	−0.0199	−0.0205	−0.0205	2.0	−1.0	3.0
2	4	−0.0282	−0.0280	−0.0264	1.0	−1.0	0.0
2	5	−0.0349	−0.0341	−0.0311	1.0	−1.0	0.0
3	2	−0.0086	−0.0081	−0.0079	7.0	7.0	7.0
3	3	−0.0162	−0.0153	−0.0151	5.0	−1.0	4.0
3	4	−0.0252	−0.0237	−0.0220	3.0	−1.0	1.0
3	5	−0.0326	−0.0301	−0.0273	3.0	−1.0	1.0
4	2	−0.0081	−0.0076	−0.0076	10.0	10.0	10.0
4	3	−0.0145	−0.0120	−0.0130	9.0	9.0	9.0
4	4	−0.0220	−0.0197	−0.0187	6.0	−2.0	6.0
4	5	−0.0299	−0.0268	−0.0244	4.0	−2.0	2.0
5	2	−0.0077	−0.0073	−0.0083	12.0	12.0	13.0
5	3	−0.0140	−0.0113	−0.0126	12.0	12.0	13.0
5	4	−0.0198	−0.0160	−0.0171	10.0	6.0	11.0
5	5	−0.0272	−0.0237	−0.0219	6.0	−1.0	7.0

[1] distance between tunnel axes. [2] soil coverage. [3] (+) towards second cavity (−) towards first cavity.

Figures 9 and 10 show their behavior according to the depth and distance between tunnels ratio. Similar behavior for the maximum settlement can be observed in all methodologies, showing a decrease as the ratio distance between tunnels/depth (L/C) increases.

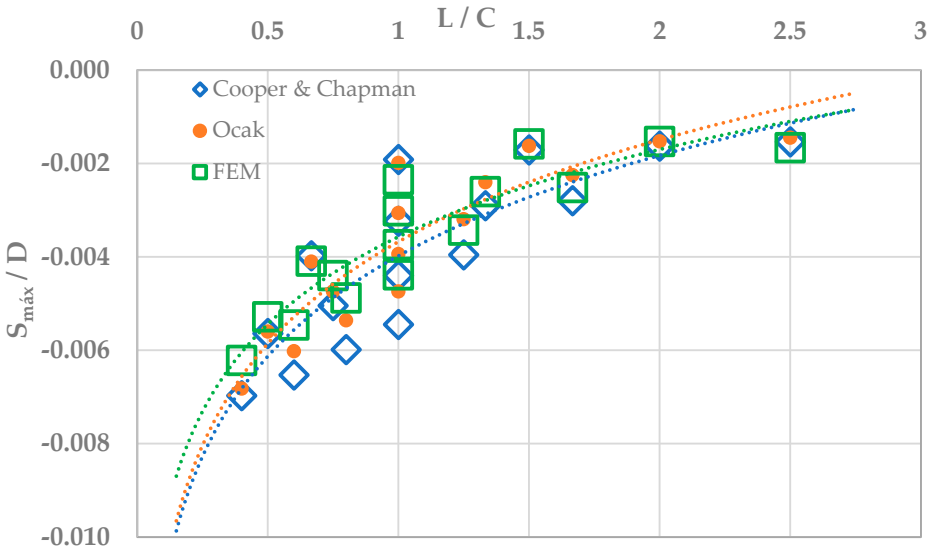

Figure 9. Maximum settlement for different methodologies.

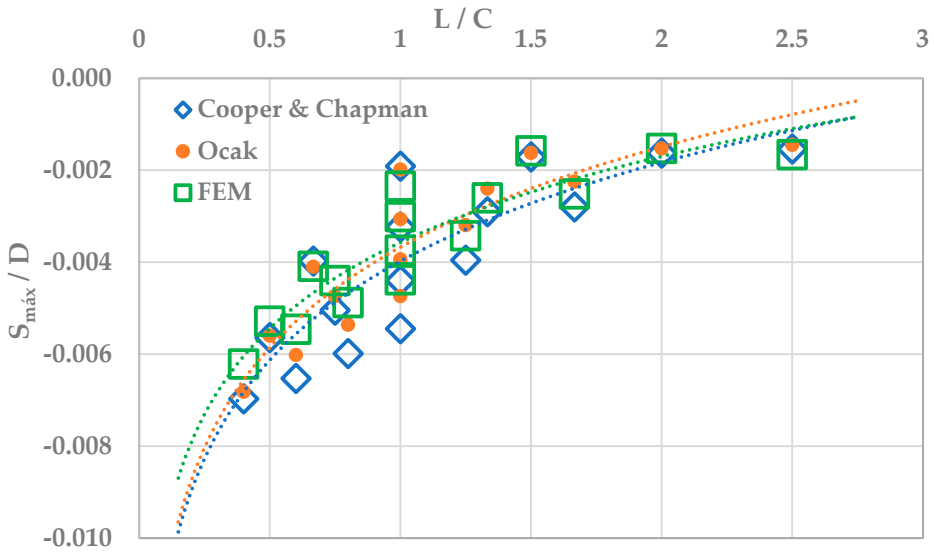

Figure 10. Eccentricity (e_{Smax}) for different methodologies.

The eccentricity shows an inverse relation with the ratio L/C, increasing with the increase in such ratio and seeming to converge to 3 as $L/C \rightarrow \infty$; nevertheless, for smaller ratios, Ocak's methodology presents an eccentricity towards the 1st cavity while O'Reilly and New behave as the FEM data with eccentricity towards the second cavity.

To evaluate the settlement trough width, it was necessary to apply the concept of the second derivative also to Cooper and Chapman's [16] methodology as done for the FEM curve and compare the ratio i_2/i_1 with the multiplying factor defined by Ocak [17], Table 6 presents the values that define the trough width and Figure 11 their variation with the ratio C/D.

Table 6. Numerical analyses settlement trough width parameter "*i*".

Geometric Configuration		Cooper and Chapman			Ocak			FEM [3]		
C [2]/D	L [1]/D	i_1 (m)	i_2/i_1	[3] i_2 (m)	i_1 (m)	i_2/i_1	i_2 (m)	i_1 (m)	i_2/i_1	i_2 (m)
2	2	4.26	1.00	4.25	4.26	1.35	5.74	5.26	1.06	5.55
2	3	4.26	1.00	4.25	4.26	1.28	5.44	5.24	1.04	5.43
2	4	4.24	1.12	4.75	4.24	1.26	5.35	5.25	1.04	5.47
2	5	4.25	1.00	4.25	4.25	1.26	5.35	5.25	1.04	5.44
3	2	7.62	0.98	7.50	7.62	1.18	8.97	7.32	1.08	7.89
3	3	7.63	0.98	7.50	7.63	1.14	8.68	7.31	1.04	7.59
3	4	7.60	0.99	7.50	7.60	1.12	8.55	7.31	1.03	7.56
3	5	7.60	0.99	7.50	7.60	1.12	8.52	7.29	1.03	7.51
4	2	11.37	1.01	11.50	11.37	1.08	12.31	9.45	1.07	10.15
4	3	11.37	1.01	11.50	11.37	1.07	12.20	9.44	1.04	9.85
4	4	11.38	1.01	11.50	11.38	1.06	12.09	9.45	1.04	9.80
4	5	11.38	1.01	11.50	11.38	1.06	12.06	9.32	1.08	10.06
5	2	15.39	1.01	15.50	15.39	1.02	15.75	11.72	1.06	12.43
5	3	15.41	1.01	15.50	15.41	1.03	15.84	11.80	1.04	12.25
5	4	15.44	1.00	15.50	15.44	1.03	15.84	11.75	1.05	12.38
5	5	15.45	1.00	15.50	15.45	1.02	15.81	11.11	1.05	11.66

[1] distance between tunnel axes. [2] soil coverage. [3] second derivatives from first-order finite difference.

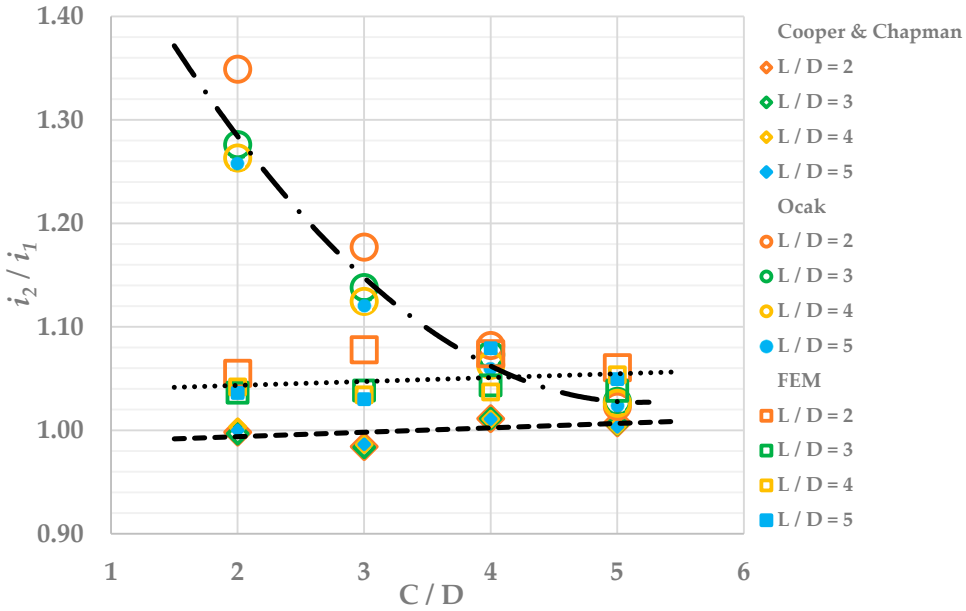

Figure 11. Trough width parameter ratio i_1/i_2 for different methodologies.

The ratio of the trough width parameter (i_1/i_2) for Cooper and Chapman [16] methodology and the FEM curves presents the same pattern of slightly linear increase with depth showing little or no dependence on the distance between tunnels, which may be explained by the fact that both are based on numerical analyses.

On the other hand, Ocak's methodology, based on field measurements, varies significantly with the depth of the tunnels, although showing little influence from the distance between cavities.

5. Conclusions

The maximum displacement, for both settlement adjustment semi-empirical methodologies and numerical analysis, presents similar behavior with the ratio distance between tunnels/depth, decreasing with the increase in such ratio.

The maximum settlement eccentricity also shows, for all the methodologies, similar behavior with the distance between tunnels/depth ratio (L/C), increasing with the increase in such ratio and seeming to converge to 3 as $L/C \rightarrow \infty$; nevertheless, for smaller ratios, Ocak's methodology presents an eccentricity towards the first cavity while Chapman and Cooper behave as the FEM data with eccentricity towards the second cavity.

The behavior of Ocak's second tunnel trough width parameter (i) presents a considerable variation with the ratio depth/tunnel diameter (C/D). In contrast, the results from Cooper and Chapman [16], as well as the ones from FEM numerical analysis, show a similar pattern with a slightly linear increase with depth not depending much on the distance between tunnels, which may be explained by the fact that both are based on numerical analyses, although settlement data from three stretches of the London subway have validated the semi-empirical formulation.

The Gaussian settlement trough is based on parameters such as the volume loss and the point of inflection (i), both empirical values. Nevertheless, the elastic parameters for numerical analysis can be obtained from unconfined compression tests on samples from the early design field investigations.

The FEM analysis, even using a simple linear elastic constitutive model, has shown consistent results with the semi-empirical methodologies validated by field data. Therefore, it should be considered as a more flexible tool to calculate the settlement trough, once besides using parameters from laboratory data and allowing the simulation of media heterogeneity and anisotropy can incorporate the consolidation process in the presence of water.

It must be emphasized that numerical methods demand a reasonable interpretation of field and laboratory test results and a careful and responsible choice of constitutive models and parameters.

It is intended to expand this study by exploring other geometric configurations and dimensions and constitutive models besides validation with field data from the literature. This shall bring a better understanding of the influence of the first tunnel excavation in the settlement trough of the second tunnel.

Author Contributions: Conceptualization: M.d.C.R.C. Methodology: M.d.C.R.C. Software: (data processing) M.C.d.S.J. Validation: W.N.R. Formal analysis: W.N.R. Investigation: M.C.d.S.J. and M.d.C.R.C. Data curation: M.C.d.S.J. Writing—original draft preparation: M.d.C.R.C.; Writing—review and editing: M.d.C.R.C. and W.N.R. Visualization: M.d.C.R.C. All authors have read and agreed to the published version of the manuscript.

Funding: This research received no external funding.

Data Availability Statement: Most of the pertinent data have been presented in the graphs and tables, nevertheless the raw data from the numerical analyses can be provided upon request.

Conflicts of Interest: The authors declare no conflict of interest.

References

1. Peck, R.B. Deep excavation and tunneling in soft ground. In Proceedings of the 7th International Conference on Soil Mechanics and Foundation Engineering, Mexico City, Mexico, 1969; Volume 3, pp. 225–290.
2. Attewell, P.; Farmer, I.; Glossop, N. Ground deformation caused by tunneling in a silty alluvial clay. *Ground Eng.* **1978**, *11*, 32–41.
3. Atkinson, J.H.; Potts, D.M. Subsidence above shallow tunnels in soft ground. *J. Geotech. Eng. Div.* **1977**, *103*, 307–325. [CrossRef]
4. Clough, G.W.; Schmidt, B. Design and Performance of Excavations and Tunnels in Soft Clay. *Dev. Geotech. Eng.* **1981**, *20*, 567–634.
5. O'Reilly, M.P.; New, B.M. Settlements above Tunnels in the United Kingdom—Their Magnitude and Prediction. In Proceedings of the Third International Symposium on Tunneling (Tunnelling '82), Brighton, UK, 7–11 June 1982; pp. 173–181.
6. Mair, R.J. Geotechnical aspects of soft ground tunneling. In Proceedings of the International Seminar on Construction Problems in Soft Soils, Sentosa, Singapore, 1–3 December 1983.
7. Mair, R.J.; Taylor, R.N. Bored tunneling in the urban environment. State-of-the-art Report and Theme Lecture. In Proceedings of the Fourteenth International Conference on Soil Mechanics and Foundation Engineering, Hamburg, Germany, 6–12 September 1997; pp. 2353–2385.
8. New, B.M.; O'Reilly, M.P. Tunneling induced ground movements; predicting magnitude and effects. In Proceedings of the 4th International Conference on Ground Movements and Structures, Cardiff, UK, 8–11 July 1991; pp. 671–697.
9. Terzaghi, K. Shield tunnels of the Chicago subway. *J. Boston Soc. Civ. Eng.* **1942**, *29*, 163–210.
10. Moretto, O. Discussion on Deep excavations and tunneling in the soft ground. In Proceedings of the 7th International Conference on Soil Mechanics and Foundation Engineering, Mexico City, Mexico, 1969; Volume 3, pp. 311–315.
11. Cording, E.J.; Hansmire, W.H. Displacement around soft ground tunnels. In Proceedings of the Pan American Conference Soil Mechanics and Foundation Engineering, Buenos Aires, Argentina, 17–22 November 1975; Volume 4, pp. 571–633.
12. Akins, K.P.; Abramson, L.W. Tunneling in residual soil and rock. In Proceedings of the Rapid Excavation and Tunneling Conference, Chicago, IL, USA, 12–16 June 1983; Volume 1, pp. 3–24.
13. Chapman, D.N.; Rogers, C.D.F.; Hunt, D.V.L. Investigating the settlement above closely spaced multiple tunnel constructions in soft ground. In *Chapter of the book (Re) Claiming the Underground Space*; Publisher Routledge: Amsterdam, The Netherland, 2003; Volume 2, pp. 629–635.
14. Addenbrooke, T.I.; Potts, D.M. Twin tunnel construction—Ground movements and lining behavior. In *Geotechnical Aspects of Underground Construction in Soft Ground*; Balkema, A.A., Ed.; Brookfield: Rotterdam, The Netherlands, 1996; ISBN 90 5470 856 8.
15. Addenbrooke, T.I.; Potts, D.M. Twin tunnel interaction: Surface and Subsurface Effects. *Int. J. Geomech.* **2001**, *1*, 249–271. [CrossRef]
16. Cooper, M.L.; Chapman, D.N.; Rogers, C.D.F.; Chan, A.H.C. Movements in the Piccadilly Line tunnels due to the Heathrow Express construction. *Géotechnique* **2002**, *52*, 243–257. [CrossRef]
17. Ocak, I. A new approach for estimating of settlement curve for twin tunnels. In Proceedings of the World Tunnel Congress, Iguassu Falls, Brazil, 9–15 May 2014.
18. Qi, X.H.; Zhou, W.H. An efficient probabilistic back-analysis method for braced excavations using wall deflection data at multiple points. *Comput. Geotech.* **2017**, *85*, 186–198. [CrossRef]
19. Zhou, W.; Tan, F.; Yuen, K. Model updating and uncertainty analysis for creep behavior of soft soil. *Comput. Geotech.* **2018**, *100*, 135–143. [CrossRef]
20. Suwansawat, S.; Einstein, H.H. Artificial neural networks for predicting the maximum surface settlement caused by EPB shield tunneling. *Tunn. Undergr. Space Technol.* **2006**, *21*, 133–150. [CrossRef]

21. Chen, R.P.; Zhang, P.; Kang, X.; Zhong, Z.Q.; Liu, Y.; Wu, H.N. Prediction of maximum surface settlement caused by earth pressure balance (EPB) shield tunneling with ANN methods. *Soils Found.* **2019**, *59*, 284–295. [CrossRef]
22. Cheng, Z.L.; Zhou, W.H.; Ding, Z.; Guo, Y.X. Estimation of spatiotemporal response of rooted soil using a machine learning approach. *J. Zhejiang Univ. SCIENCE A* **2020**, *21*, 462–477. [CrossRef]
23. Cheng, Z.L.; Zhou, W.H.; Garg, A. The genetic programming model for estimating soil suction in shallow soil layers in the vicinity of a tree. *Eng. Geol.* **2020**, *268*, 105506. [CrossRef]
24. Gao, Y.; Liu, Y.; Tang, P.; Mi, C. Modification of Peck Formula to Predict Surface Settlement of Tunnel Construction in Water-Rich Sandy Cobble Strata and Its Program Implementation. *Sustainability* **2022**, *14*, 14545. [CrossRef]
25. Zhao, W.; Jia, P.J.; Zhu, L. Analysis of the Additional Stress and Ground Settlement Induced by the Construction of Double-O-Tube Shield Tunnels in Sandy Soils. *Appl. Sci.* **2019**, *9*, 1399. [CrossRef]